CRITICAL COMPARISON OF START-STOP ASYNCHRONOUS MOTOR USED FOR INDUSTRIAL CONVEYOR

Geani-George LAZĂR[1], Lucian PETRESCU[2], Emil CAZACU[3], Aurel CHIRILĂ[4], Dragoș DEACONU[5], Maria-Cătălina PETRESCU[6]

Asynchronous motors are very robust constructive machines, and consequently are widely used in various industrial applications. In this sense, conveyor belts used for transportation and packaging of metal cans represent a typical load of these motors. Within this conveyor belt, the stop and start sequence of the induction motor plays an essential role in the electric drive system design. The paper proposed a critical comparative study of the start and stop cycle for a low-voltage 3-kW asynchronous motor by two different energizing procedures. Thus, the comparison is performed considering the motor classic star-delta starting method and the utilization of a controlled variable frequency drive (VDF). The results highlight the major advantages of using adjustable-speed drives in all terms of the connecting and disconnecting process.

Keywords: asynchronous motor, star-delta connection, industrial conveyor, variable frequency drive

1. Introduction

Induction motors are essential devices in any modern electrical installation [1-3]. In various forms and constructive solutions, these motors are easy to produce, to maintain and additionally their manufacturing costs are significantly reduced. Considering aspects of sustainability and energy efficiency, these equipments represent the ideal solution in a multitude of situations [4,5]. They can

[1] PhD Student, Dept. of Electrotehnics, University POLITEHNICA of Bucharest, Romania, e-mail: lazargeani27@gmail.com
[2] Associate Professor, Dept. of Electrotehnics, University POLITEHNICA of Bucharest, Romania, e-mail: lucian.petrescu@upb.ro
[3] Prof., Dept. of Electrotehnics, University POLITEHNICA of Bucharest, Romania, e-mail: emil.cazacu@upb.ro
[4] Associate Professor, Dept. of Electrical Machines, Drives and Materials, University POLITEHNICA of Bucharest, Romania, e-mail: aurel.chirila@upb.ro
[5] Prof., Dept. of Electrical Machines, Drives and Materials, University POLITEHNICA of Bucharest, Romania, e-mail: dragos.deaconu@upb.ro
[6] Lecturer, Dept. of Electrotehnics, University POLITEHNICA of Bucharest, Romania, e-mail: catalina.petrescu@upb.ro

be found in many applications fields from the textile industry [6] to the oil and gas extraction industry [7].

A particularly important aspect of these motors is their ability to numerously start and stop. Thus, for a conveyor belt, used in the food industry, the presence of an asynchronous motor with a very high number of start-stops represents an essential link in the operation of these enterprises [8, 9]. The pallet transport and handling line is structured in two main areas (pallet loading area, pallet packing and unloading area) and a secondary area (rest area). In the loading area there are two palletizers by means of which the boxes are placed on the pallets, in the rest of the area there is the trolley, which transports the pallets. In the packing and unloading area there are the tying machine, the wrapping machine, and the conveyors with which the pallets are transported to the pick-up point [10].

A variable frequency drive (VFD) is an electrical device used to control the rotational speed of an AC electric motor by adjusting the frequency of the electrical power supplied to the motor [11]. A variable frequency drive works by converting input alternating current power to direct current using a diode bridge rectifier, which then passes through a filter and smoothing block to be converted back to alternating current power by via an inverter that controls the voltage and frequency sent to the motor via high-speed transistors [12, 13].

This paper aimed to carry out a comparative study between the start-stop features of these motors in the conveyor belt with the classic solution of the star-delta connection, respectively with the help of a variable frequency drive (VFD).

2. General characteristics of the devices

The load of the investigated system is driven by a 3-kW wound rotor induction motor. It is energy efficient and provides sufficient characteristics to drive the conveyor belt. In Table 1 are presented the main characteristic of this motor. These data are also implemented in the simulation part of the paper (illustrated in the 3rd section of the paper).

Table 1

Main characteristics of the studied asynchronous motor

Motor data	Value
Rated power: P_n	3 kW
Rated current I_n	8 A
Pole pair number: p	2
Rated frequency: f_n	50 Hz
Rated voltage: U_n	380 V
Rated speed: n_n	1450 [rpm]
Rated power factor	0.88

Analysis of system operation with repeated starts and stops requires the use of a VFD. In the case of here presented application, the adjustable-speed drive is a Fuji model, with the identification code FRN0011C2S-4E, from the Mini C2 range [14]. Its main functional features are shown in Table 2. These are correlated with the induction motor data.

Table 2

Main characteristics of the studied asynchronous motor

VFD Model FRN0011C2S-4E		
Rated power of the controlled motor [kW]	3.7 / 4.0	
VFD output values	Rated power [kW]	3.7 / 4
	Rated voltage [V]	380 - 480
	Rated current [A]	10.5
VFD input values	Rated power [kW]	2.5
	Rated voltage [V]	380 - 480
	Rated current [A]	7.3

3. Direct connection of the motor

Star-delta (or wye-delta) starting of asynchronous motors is a classic energizing method, studied comprehensively examined [15-17], and implemented in innumerous functional systems. In this section, starting from the diagram in Fig. 1, implemented in Matlab Simulink [18], the simulation of the star-delta starts of the analyzed induction motor was completely investigated.

On the left side one can find the power supply area, where after 5 ms the motor is connected to star configuration. This lasts up to one second, then in the interval of 1.11 - 1.5 seconds, the transition to the delta connection is performed. At the bottom of the schematic, one can notice the scopes where the line and phase voltages will be visualized (Line and phase voltage display) Supplementary, the variation of the torque (Torque Evolution) and the motor speed of rotation (RPM Evolution) are also illustrated. In addition, by means of a Bus Selector type block, the visualization of the stator current waveforms (Evolution of stator currents) was enabled.

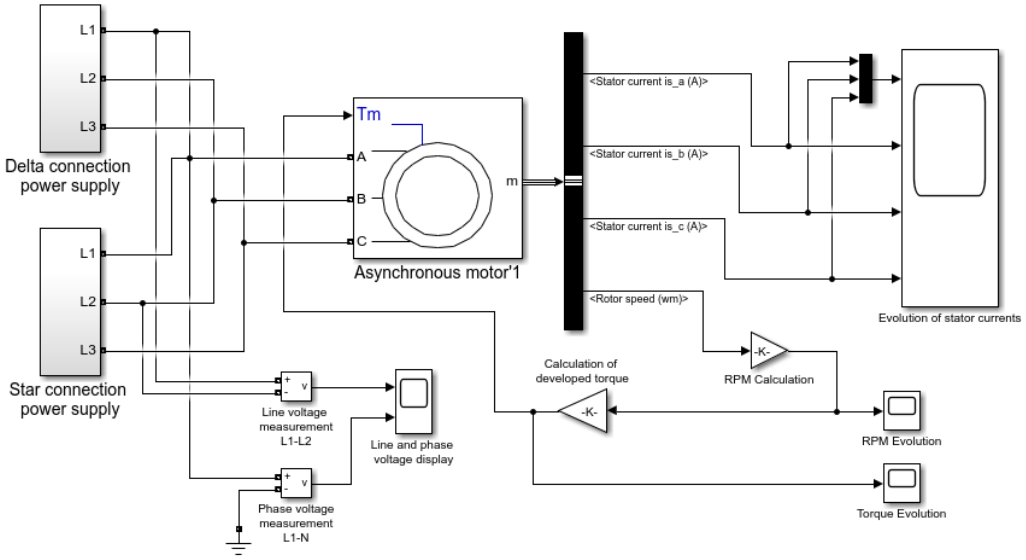

Fig. 1. Simulation scheme of the star-delta connection of the asynchronous motor.

After the simulation, the variations of the analyzed quantities can be observed. Accordingly, Fig. 2 presents the line voltage (the phase voltages have a similar evolution).

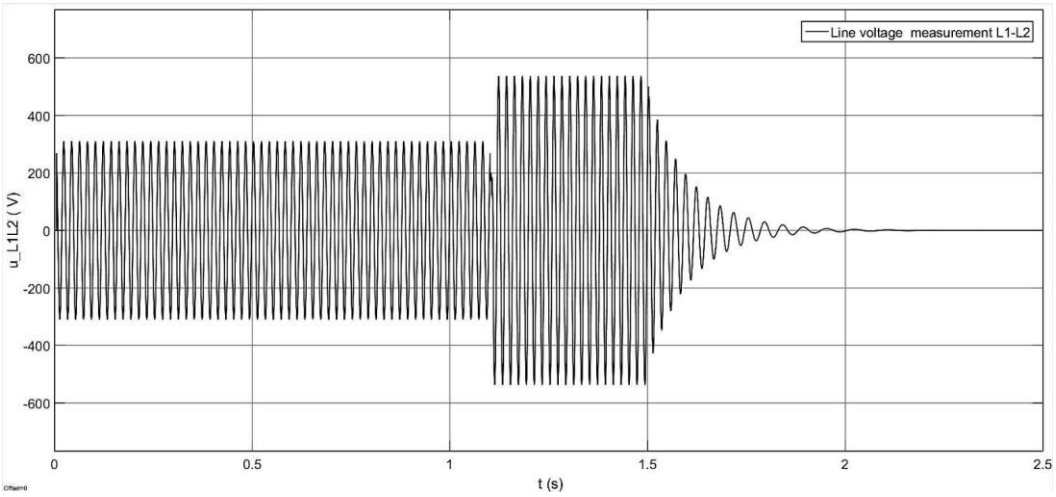

Fig. 2. Line voltage variation.

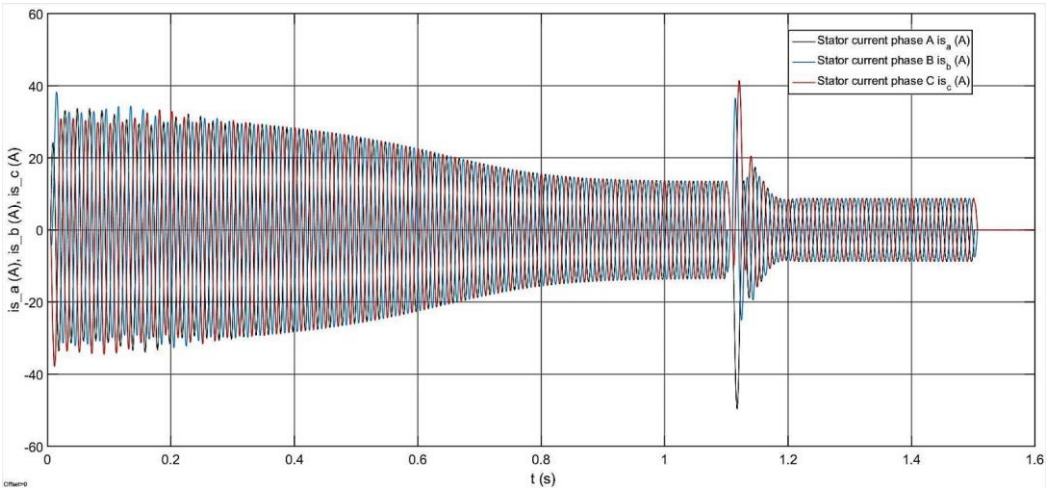

Fig. 3. Variation of stator currents.

From the evolution of the stator currents, one can remark that the value of the absorbed current at the energizing instant is about 4 times higher than the value of the rated motor current (Fig. 3). When the source is coupled for the delta connection power supply, the current reaches the value corresponding to the star connection, but the interval of the current high value is much smaller than in the previous case. The period of this transient regime also depends on the mode of switching between the two states. In the case of these simulations, an average time was chosen, very close to that encountered in real installations.

The time chosen for the star-delta transition (one second) is also determined by the motor rated speed. In Fig. 4 the variation of the rotation speed over the range of star start, delta connection and then free stop is captured. The torque variation on the same scenario can be seen in Fig. 5.

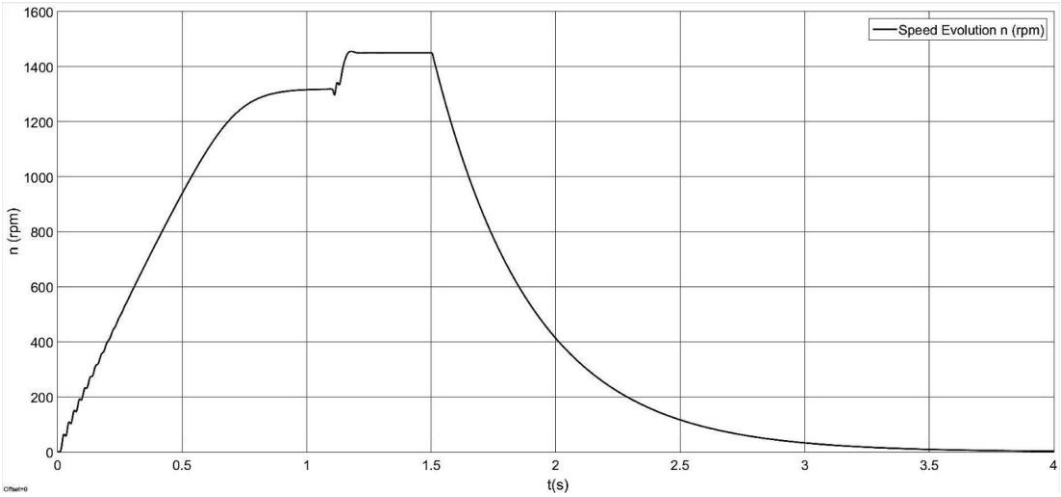

Fig. 4. Induction motor speed evolution.

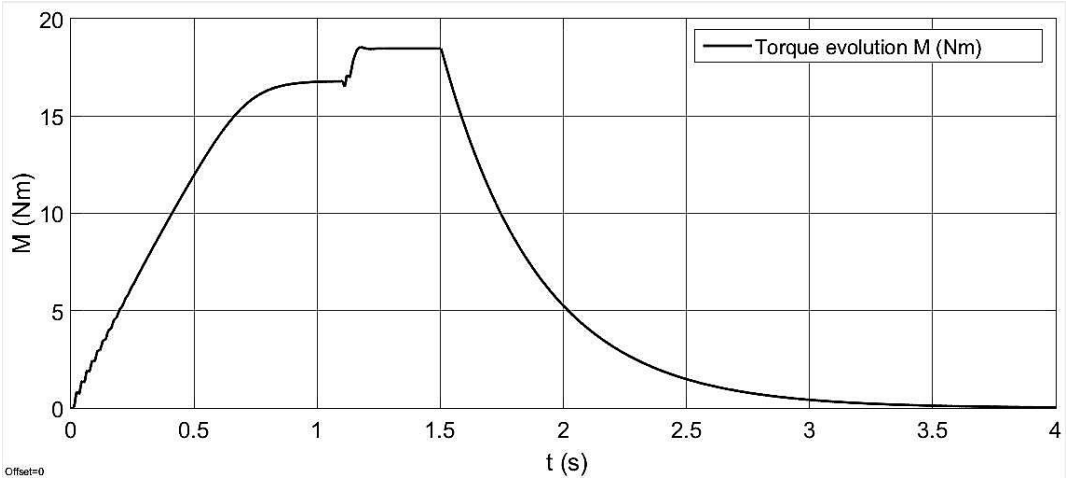

Fig. 5. Induction motor torque evolution.

4. Variable frequency drive connection of the motor

Using the previously described devices, an experimental stand was set-up in which the starting and stopping processes of the wound rotor induction motor were also examined by means of the of a variable-frequency drive (VFD) usage. Fig. 6 shows the block diagram based on which the connections of the acquisition system were established, a system that acquires the analyzed waveforms at 64 kHz frequency (f_{DAQ} = 64 kHz). It consists of three current and voltage measuring instruments at the converter and motor. The acquired values are the instantaneous one.

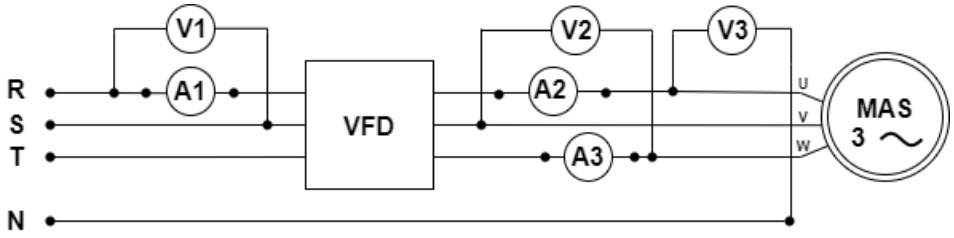

Fig. 6. Block diagram for measuring parameters.

Results obtained using the frequency inverter produced by FUJI Electric at a reference frequency of 50 Hz and acceleration time of 3s are presented in Fig. 7.

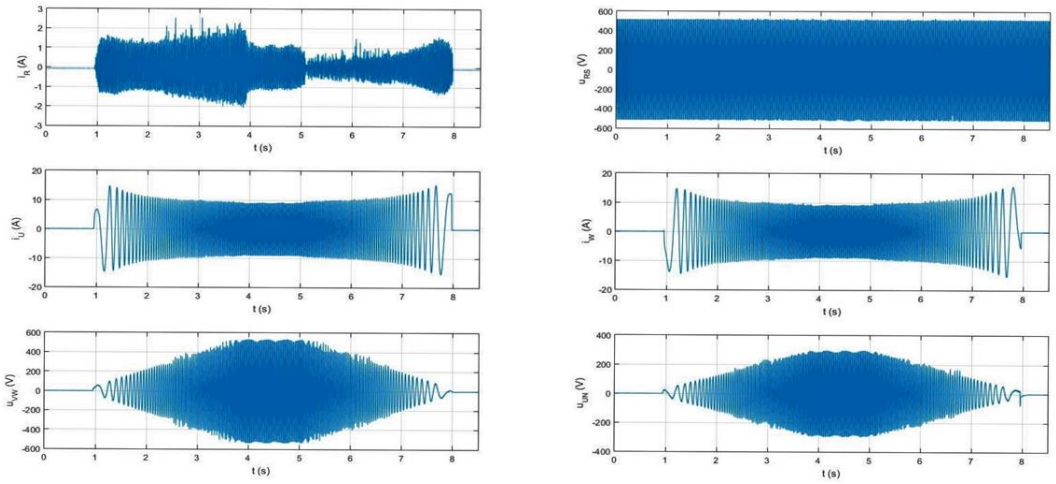

Fig. 7. Variation of the acquired quantities (current at the inverter input i_R (A), line voltage at the inverter input (u_{RS} (V), line currents at the inverter output i_U (A), i_W (A), line voltage and phase voltage at the inverter output u_{VW} (V), u_{UN} (V)).

The acquisition of these quantities was influenced by transient disturbances and electrical noise. To reduce these perturbations is possible by using shielding methods. The most common one adopted in many practical cases is the usage of shielded cables by tying the cable braid to ground. In this application, the isolation of the equipment power supply in the system was done by using shielded cables and their connecting their braid to the grounding at one end only. Thus, the appearance of a ground loop was avoided. To observe as accurately as possible the variation of the quantities we applied a numerical filtering method, namely the moving average [19] (Fig. 8).

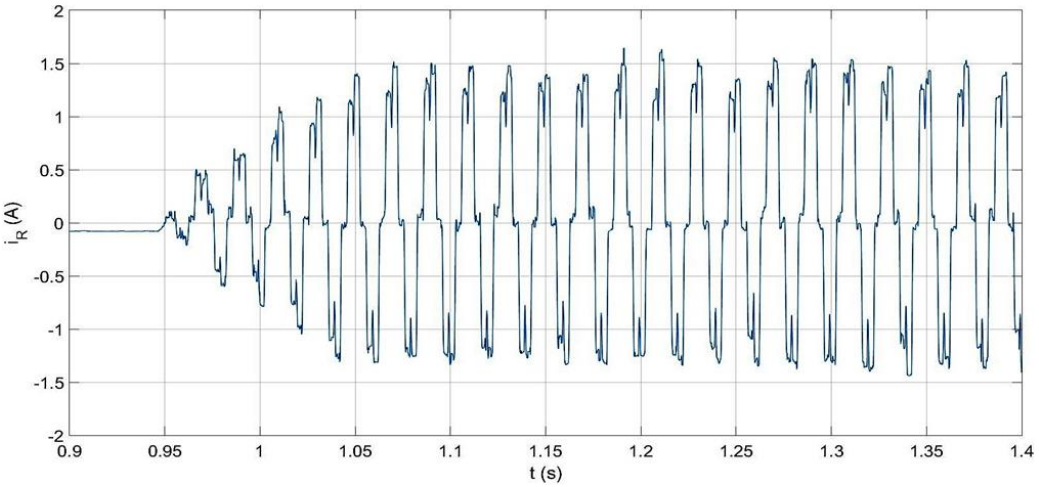

Fig. 8. Evidence of the variation of the current absorbed by the inverter at start-up.

The evolution of the input current to the frequency inverter can be seen to be non-sinusoidal, which is influenced by the presence of the three-phase rectifier in the uncontrolled bridge (Fig. 9). It can be seen how at the start-up and shutdown instant, at a low frequency, the value of the absorbed current is higher compared to the rated one (Fig. 10).

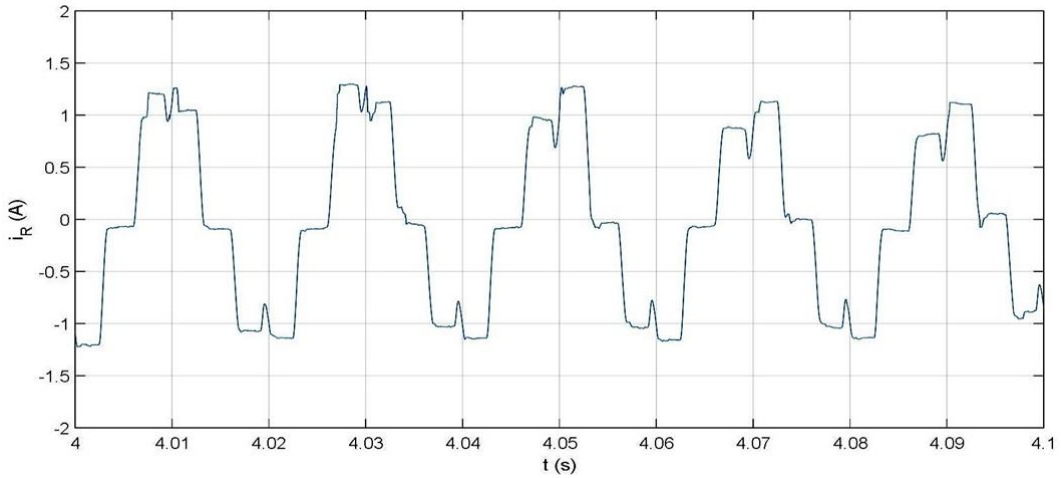

Fig. 9. Nonsinusoidal current absorbed by the inverter during operation at a frequency of 50 Hz.

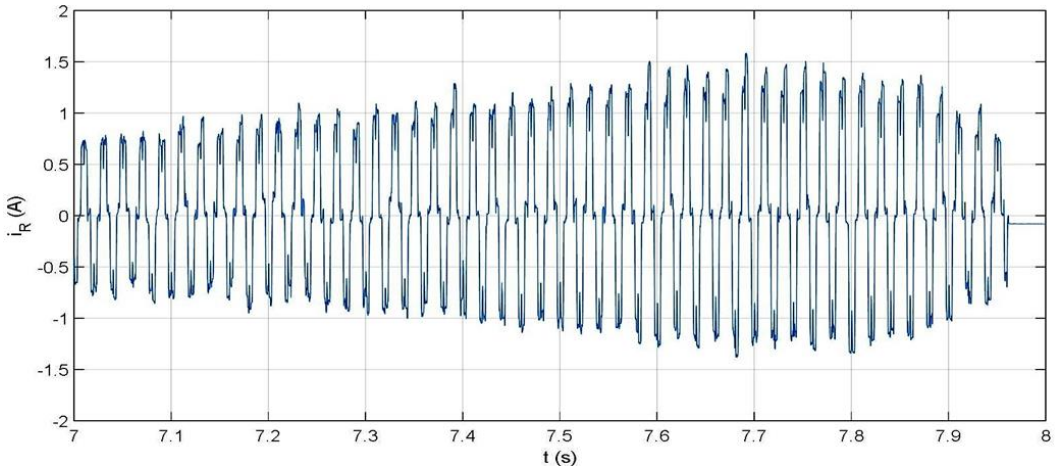

Fig. 10. Variation of the current absorbed by the inverter at shutdown.

Analyzing the evolution of the current at the frequency inverter output, we can notice that at the starting instant it does not exhibit a sudden increase. This is mainly caused due to the acceleration ramp (Fig. 11). The evolution of the output current has also higher values when the frequency of the supply voltage is lower. That can be observed both when the motor switches on and off (Fig. 12).

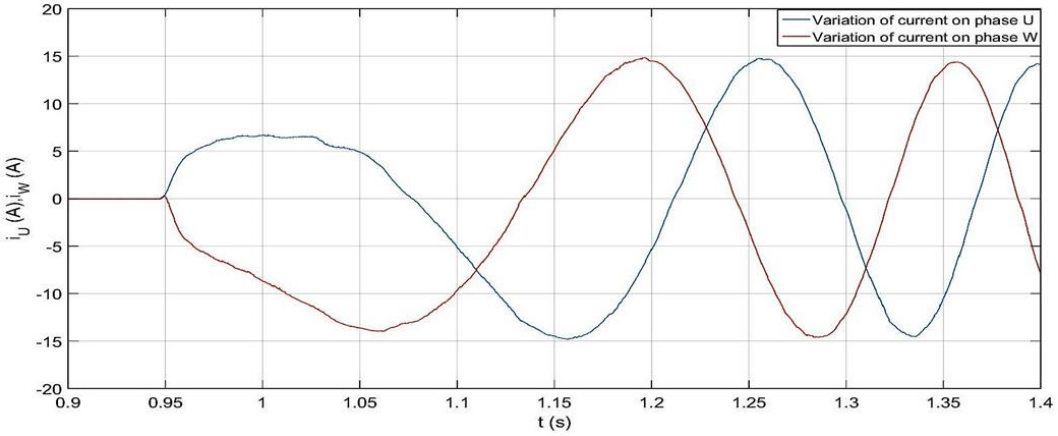

Fig. 11. Variation of the current on the U and W phases at the inverter output at start-up.

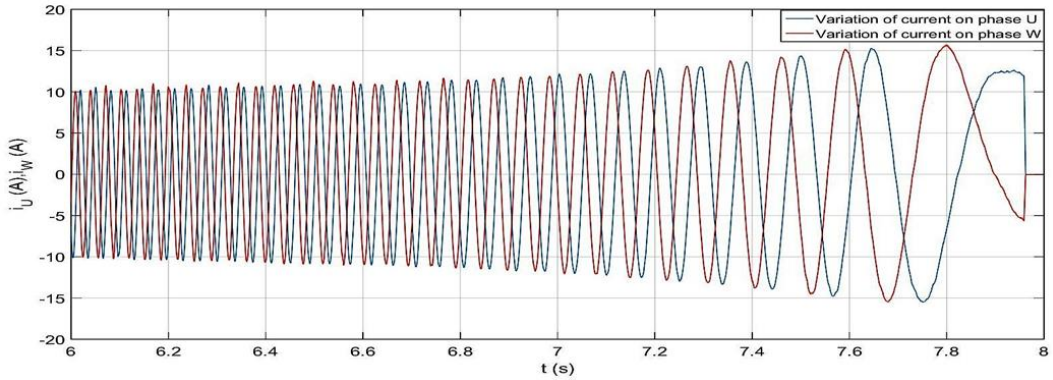

Fig. 12. Variation of the current on the U and W phases at the inverter output at the time of shutdown.

The voltage at the VDF terminals has a perfectly sinusoidal shape during motor normal operation. Analyzing the evolution of both line and phase voltages at the inverter output, it is remarked that their values increase proportionally to its frequency (Fig. 13). This evolution shows that the inverter is controlled by the constant voltage to frequency ratio method (Fig. 14).

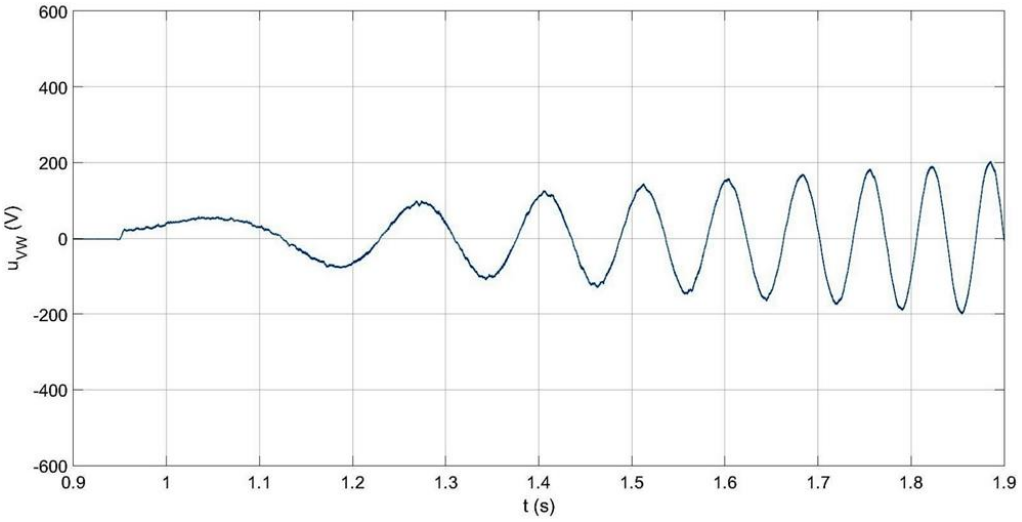

Fig. 13. Voltage variation at the inverter output at start-up.

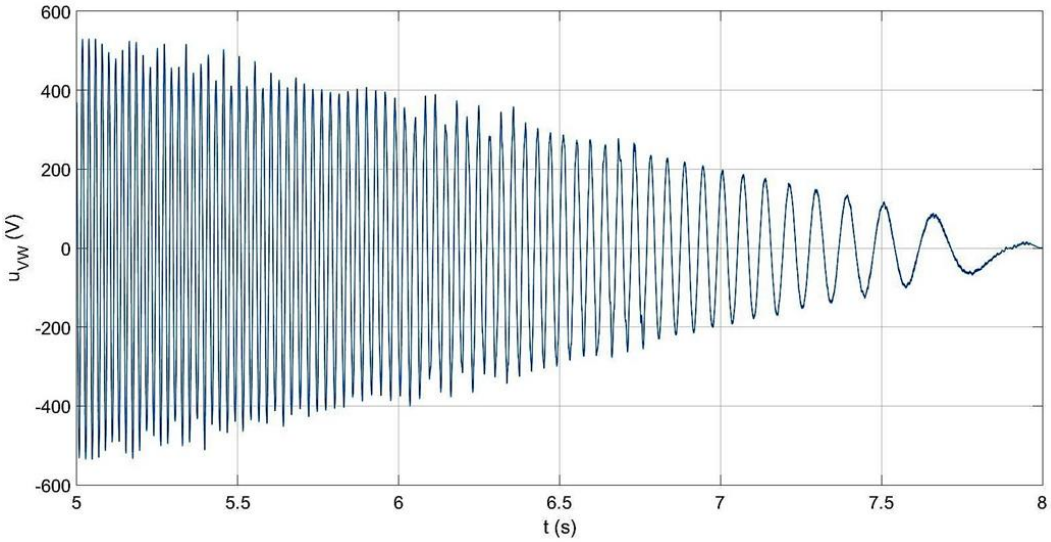

Fig. 14. Voltage variation at the output of the converter at the time of shutdown.

5. Conclusions

The increasingly widespread use of induction motors in the large variety of industrial applications leads to the continuous search for their best possible practical usage solutions both in terms of speed or torque control and high energy efficiency. The repeated start-up cycles faced by such a motor used on a conveyor belt application in the food industry were investigated and critically analyzed. The results obtained by simulation in Matlab, for these two actions (start-stop) were compared with the experimental data using a variable frequency drive. In the

simulation, there were used the parameters of the same engine as the one in the experimental part, thus highlighting the advantage brought by the VFD in the case of repeated starts and stops.

As expected, using a VFD brings several benefits:

• Easy starting capability, thus significantly reducing the starting (inrush) current of the motor, and consequently, reducing the electrical and mechanical stress on the motor, and improving its reliability.

• Significant reduction of the machine's energy consumption with the help of adequate control.

• Improving the power factor of the entire drive system, including the VFD and motors.

• Monitoring and measuring the system performance from an electrical point of view.

The used Fuji VFD has low cost, high availability in the market, and is also easy to use. The choice of using a VFD is necessary because the transport of the pallet must be carried out in optimal conditions in order not to have a sudden start or stop of the trolley and it is also required to stop at a fixed point.

R E F E R E N C E S

[1]. *K. Dambrauskas, J. Vanagas, S.s Bugenis, T. Zimnickas, A. Kalvaitis*, "Methodology for Asynchronous Motor Impedance Measurement by Using Higher Order Harmonics", Energies 2020, 13, 2541, pp. 1-13, doi:10.3390/en13102541.

[2]. *X. Zhao, P. Qin, Z. Tang*, "Equivalent Inertia Estimation of Asynchronous Motor and Its Effect on Power System Frequency Response", Energies 2022, 15, 8350, pp. 1-16, https://doi.org/10.3390/en15228350.

[3]. *B. F. Venescu, A. F. Bucsa, M. Iordache,* Analysis of the permanent sinusoidal regime of the asynchronous motor of the primary circuit pumps from a nuclear power plant, U.P.B. Sci. Bull., Series C, Vol. **83**, Iss. 2, 2021.

[4]. *Z. Li, S. Che, P. Wang, S. Du, Y. Zhao, H. Sun, Y.Li,* "Implementation and analysis of remanufacturing large-scale asynchronous motor to permanent magnet motor under circular economy conditions", Journal of Cleaner Production, 294 (2021) 126233, https://doi.org/10.1016/j.jclepro.2021.126233.

[5]. *H. Uzun, O. Akar, A. Demirci, M.C. Akuner, U.K. Terzi*, "Analyzing High Efficiency Asynchronous Motors Using Scalar Control Technique", Balkan Journal of Electrical and Computer Engineering, 2018, pp. 23-26, 10.17694/bajece.410219.

[6]. *N. Pirmatov, A. Panoev*, "Frequency control of asynchronous motors of looms of textile enterprises", E3S Web of Conferences 216, 01120 (2020), pp. 1-4, https://doi.org/10.1051/e3sconf/202021601120.

[7]. *M. Y. Khan, P. S. Rao, B.S. Pabla, S Ghotekar*, "Innovative biodiesel production plant: Design, development, and framework for the usage of biodiesel as a sustainable EDM fluid", Journal of King Saud University - Science, **34** (6), 2022, 102203 pp. 1-10, https://doi.org/10.1016/j.jksus.2022.102203.

[8]. *G. Gandhi, G.S. Sharma*, "The pallet conveyor system application in the industrial lines-a new design system with improvement of productivity", International Journal of Mechanical and

Production Engineering Research and Development, 2019, vol. 9, no. 3, pp. 257-266, 10.24247/ijmperdjun201929.

[9]. *L. Jakubovičová, P. Kopas, M. Vaško, M. Handrik*, "Technical solution of the modern conveyor system", IOP Conf. Ser.: Mater. Sci. Eng. 1199 012031, 2021, pp. 1-10, DOI: 10.1088/1757-899X/1199/1/012031.

[10]. *A. B. Singh, V. Rukkumani, P. Manju, R. Srinivasan, A. S. Jothi*, "A. Review on Conveyor Systems and Thermography", Journal of Engineering Science and Technology Review, 2020, vol. 13, no. 1, pp. 171-192, DOI:10.25103/Jestr.131.23.

[11]. *H. Bounoua, A. Bounoua*, "The utilization of the PWM inverter feeding in the asynchronous motor command", Electronic Journal Technical Acoustics, 2004, vol. 8, pp. 1-11.

[12]. *X. Hong, C. Zhu, S. An, Y. Zha*, "Simulation analysis of transient output characteristics of inverter with asynchronous motor load based on second-order filtering link", Sustainable Energy Technologies and Assessments, **49** (2022) 101725, pp. 1-14, https://doi.org/10.1016/j.seta.2021.101725.

[13]. *L. Ciufu, M. O. Popescu*, "Experimental harmonic spectrum assessment of a modern single-phase variable frequency drive designed for supplying three-phase asynchronous motors", U.P.B. Sci. Bull., Series C, Vol. **79**, Iss. 2, 2017, pp. 133-144.

[14]. ***Fuji Electric, Instruction Manual FRENIC-Mini, INR-SI47-1729A-E.

[15]. *J. A. Itajiba, C.A. C. Varnier, S. H. L.Cabral, S. F. Stefeno, V. R. Q. Leithardt, R. G. Ovejero, A. Nied, K.-C. Yow*, "Experimental Comparison of Preferential vs. Common Delta Connections for the Star-Delta Starting of Induction Motors", Energies, 2021, **14**, 1318, pp.1 – 15, https://doi.org/10.3390/en14051318.

[16]. *P. Bai, W. Nie*, "Vector control system design for asynchronous motors, 2022 8th International Symposium on Sensors, Mechatronics and Automation System", Journal of Physics: Conference Series, **2246** (2022) 012040, pp. 1-5, doi:10.1088/1742-6596/2246/1/012040.

[17]. *R. Zanasi, G. Azzone*, "Complex dynamic models of star and delta connected multi-phase asynchronous motors", International Aegean Conference on Electrical Machines and Power Electronics and Electromotion, Joint Conference, Istanbul, Turkey, 2011, pp. 195-200, doi: 10.1109/ACEMP.2011.6490594.

[18]. *** Documentation, S. (2022). Simulation and Model-Based Design. MathWorks. Retrieved from https://www.mathworks.com/products/simulink.html.

[19]. *A.I. Al-Odienat, A.A. Al-Mbaideen*, "Optimal length determination of the moving average filter for power system applications", International journal of innovative computing, information & control: IJICIC, vol. 11, No. 2, 2015, pp. 691-705.